Journal of Network Intelligence ©2024 ISSN 2414-8105 (Online)
Taiwan Ubiquitous Information Volume **9**, Number **1**, February **2024**

An Optimal Wind Turbine Control Based on Improved Chaotic Sparrow Search Algorithm with Normal Cloud Model

Qi-Peng Yang

College of Computer Science and Mathematics
Fujian Provincial Key Laboratory of Big Data Mining and Applications
Fujian University of Technology, Fuzhou 350118, China
280320910@qq.com

Chia-Hung Wang

College of Computer Science and Mathematics
Fujian Provincial Key Laboratory of Big Data Mining and Applications
Fujian University of Technology, Fuzhou 350118, China
jhwang728@hotmail.com

Thi-Kien Dao

University of Information Technology, Ho Chi Minh City 700000, Vietnam
Vietnam National University, Ho Chi Minh City 700000, Vietnam
kiendt@uit.edu.vn

Trong-The Nguyen*

University of Information Technology, Ho Chi Minh City 700000, Vietnam
Vietnam National University, Ho Chi Minh City 700000, Vietnam
thent@uit.edu.vn

Qi-Gen Zhao

College of Computer Science and Mathematics
Fujian Provincial Key Laboratory of Big Data Mining and Applications
Fujian University of Technology, Fuzhou 350118, China
1098868632@qq.com

Shu-Meng Chen

College of Computer Science and Mathematics
Fujian Provincial Key Laboratory of Big Data Mining and Applications
Fujian University of Technology, Fuzhou 350118, China
1615780452@qq.com

*Corresponding author: Trong-The Nguyen
Received May 1, 2023, revised July 28, 2023, accepted October 14, 2023.

Abstract. *This study suggests a Chaotic Sparrow Search Algorithm (CSSA) based on the Sparrow Search Algorithm (SSA) for a wind turbine generator unit's pitch controller optimal parameters. The optimal parameters set of a wind turbine pitch controller is a complex problem that needs to be tuned to archive a smooth quality performance of the outcome power operations. The CSSA is carried out with Tent chaotic mapping updating equations and a standard cloud model to avoid the original SSA algorithm drawbacks and increase quality performance to solve the optimal controller parameters. The experiments compare the CSSA against other algorithms on testing function, and the optimal pitch controller parameters demonstrate that the CSSA can solve smoothing the output power of the wind turbine unit, reducing the effect of wind speed fluctuations on the power grid.*
Keywords: Sparrow search algorithm; Tent chaotic mapping; Normal cloud model; Wind turbine generator unit.

---

1. **Introduction.** The quality of grid-connected power generation has always been a focus of industrial study in the area of wind energy production [1]. Today's two primary kinds of conventional pitch control technology are electric pitch control and hydraulic valve-controlled pitch control [2]. Due to the tiny stroke of the pitch gear and the sizeable meshing load of the pitch drive gear and ring gear, electric pitch control is possible as its development [3]. The exceedingly complicated lubrication process has made it challenging to increase the power installed power further generating [4]. The advantages of a hydraulic pitch control system, such as fast response, high control precision, and ample bearing torque, are present in valve-controlled hydraulic pitch systems [5]. Still, the oil leakage issue is challenging to address [6].

In order to increase system stability and dependability, the study's optimal control variable pitch control system utilizes an integrated design based on a metaheuristic algorithm [7]. To achieve a more stable output power from the wind turbine and to be able to effectively control the speed fluctuation under harsh operating conditions, the variable pitch optimization system was designed with the control strategy of the pitch control system in mind [8]. To maintain the wind turbine's safety, prevent and restrict overzealous shutdowns, and improve robustness and anti-interference capability [9]. It focuses on the wind power system power control issue, identifying the Wiener model of wind turbines step by step utilizing separate separable signals to estimate the output power of wind turbines more correctly [10].

Everyday optimization problems are becoming more complicated, making it harder and harder to solve them using conventional techniques [11]. Therefore, to properly handle these challenges, trustworthy optimization techniques are required [12]. The benefits of metaheuristic algorithms include flexibility, the lack of a gradient mechanism, and the ability to avoid local optima. These algorithms provide a high degree of flexibility because the input parameters and output data must be considered while handling various problems [13]. The technique, part of stochastic optimization technology, can solve problems devoid of multiple local optima without accidentally entering one. Recent years have seen a growth in research into wind turbine control thanks to artificial intelligence [14]. In essence, it combines PID control and artificial intelligence.

The sparrow optimization algorithm (SSA) [15], which takes inspiration from the predatory behavior of sparrow populations in nature, has advantages, e.g., a few control parameters and excellent implementation efficiency. However, it also suffers the same drawbacks when solving complicated engineering optimization issues [16]. For instance, as iteration progresses, the variety of the sparrow population tends to decline, and the population tends to become more homogeneous, resulting in optimal local values [1]. Numerous academics have proposed various improvement ways to address the issue that swarming intelligence optimization algorithms are prone to entering local optima and developing inadequate global search capabilities [17][18]. Chaotic sequences and Gaussian mutations were introduced into the population and perturbed to enhance the algorithm's ability to do local searches [19]. The population underwent specific conditions-based modifications after each iteration [20]. Given the significant opportunity to improve SSA's performance, we employ techniques and broaden the application of the standard cloud model presented to enhance the sparrow optimization algorithm with chaotic tent mapping.

This study provides an CSSA based on the Tent chaotic mapping and the usual cloud model to update sparrow equations using the average cloud model. The population initialization based on the Tent chaotic mapping is included to increase the algorithm's optimization efficiency and solution precision [21]. By choosing benchmark test functions and examining the optimization outcomes of single-peak, multi-peak, and composite parts using different optimization algorithms, the performance of the CSSA algorithm is confirmed. The findings demonstrate that the CSSA algorithm performs better under identical test settings regarding convergence accuracy and optimization efficiency, can swiftly depart from locally optimal solutions, and can balance global search and local development.The outstanding contributions made by this paper are as follows:

1. To enhance the population's capacity for optimization, an CSSA algorithm is proposed that takes advantage of the Tent chaotic mechanism and the regular cloud model.
2. To validate the proposed approach, we contrast it with other algorithms on the CEC2013 test set, and the CSSA algorithm's performance is certified.
3. Applied the CSSA algorithm to wind turbines' PID control parameter tuning, resulting in stable power output.

The paper is organized as follows. In section 2, we present the original SSA and discusses the operation of wind power-producing systems. In section 3, we describes CSSA based on Tent chaotic mapping and Normal Cloud Model as improvement methodologies. In section 4, we test The CSSA algorithm's performance on the CEC2013. In section 5, the method is used to manage pitch in wind energy systems and is contrasted with other algorithms. A conclusion is drawn in Section 6.

2. **Related Work.**

2.1. **Sparrow Search Algorithm.**

The sparrow search algorithm (SSA) is an emerging swarm intelligence algorithm that imitates a natural sparrow population's survival and foraging behavior [15]. The algorithm has the advantages of excellent solving ability, fast computation speed and ease of reproduction. This algorithm has been widely applied to the optimization of related parameters in practical engineering. The improved sparrow search algorithm was adapted with combined with the traditional Otsu method to deal with specific microgrid plnning optimzation.

The inspiration for the Sparrow Search Algorithm comes from the division of labor and cooperation in the communal life of sparrows. Based on the different roles sparrow plays in foraging and anti-predator activities, the algorithm is divided into three categories: discoverers, joiners, and warners [16]. The proposed sparrow algorithm should satisfy the following six principles [15].

(1) In the sparrow population, the discoverer had high fitness, was mainly responsible for finding the food-rich area within the search range, and provided the corresponding location and direction information.

(2) The identities of discoverers and joiners among individual sparrows are not fixed. Joiners become discoverers if they find better foraging areas, and a corresponding number of discoverers become joiners.

(3) The quality of foraging areas discovered by discoverers varies, and joiners follow the information of the discoverer with the highest fitness to nearby foraging areas.

(4) The sparrows that arrive first can obtain more food, so individuals that arrive later will get less food and choose to move to other areas for foraging.

(5) Each sparrow has an early warning mechanism. When a bird detects danger, it emits a warning signal. The birds must leave the current area when the signal exceeds a threshold.

(6) The sparrow population is more vulnerable when foraging on the periphery. When the early warning mechanism is triggered, sparrows gather and leave the current location to feed in a safer area.

During the algorithm search process, the positions of the discoverers are simulated according to their responsibilities. They are responsible for finding food for all the sparrows, providing an excellent foraging spot for the population, with a lot of space to search. Because the finder not only needs to meet its own food needs but also needs to detect suitable foraging areas and provide directional information to the whole population. The specific formula for updating their positions is as follows:

$$X_{i,j}^{t+1} = \begin{cases} X_{i,j}^{t} \cdot \exp\left(\frac{-i}{\alpha \cdot \text{ iter }_{\max}}\right), R_2 < ST \\ X_{i,j}^{t} + Q \cdot L, R_2 \geq ST \end{cases}, \tag{1}$$

in the Equation (1), $j = 1, 2, \ldots, d$, and $iter_{max}$ represents the algorithm's maximum number of iterations, t represents the current number of iterations, α is a random number between $(0, 1]$, the range of warning value is $R_2 \in [0, 1]$, the range of safe value is $ST \in [0.5, 1]$, Q is a random number that follows a normal distribution, and L is a $1 \times d$ matrix, where all of its entries are equal to 1.

The entrants are individuals other than the discoverer whose search direction is guided to some extent by the discoverer's location. When the entrants perceive that the discoverer has found a better foraging area, they will abandon their current place and migrate to the better foraging area in search of food. The specific location update formula is as follows:

$$X_{i,j}^{t+1} = \begin{cases} Q \cdot \exp\left(\frac{X_{\text{worst }} - X_{i,j}^{t}}{i^2}\right), \ i > \frac{N}{2} \\ X_p^{t+1} + \left|X_{i,j}^{t} - X_p^{t+1}\right| \cdot A^{+} \cdot L, \ \text{otherwise} \end{cases}, \tag{2}$$

in the Equation (2), X_{worst} represents the individual position with the worst fitness value in the $t - th$ iteration, $X_p^{(t+1)}$ represents the best discoverer position with the highest fitness value in the $t + 1 - th$ iteration, A represents a $1 \times d$ matrix, where the elements are randomly assigned to 1 or -1 values, and A^+ is the pseudo inverse of A, which is calculated as $A^+ = A^T(AA^T)^{(-1)}$.

Forewarning is a particular part of SSA; all sparrows have an early warning mechanism. They send out warning signals whenever they are aware of a danger nearby. Depending on the warning signal's strength, the sparrow will choose whether to evacuate immediately to ensure its safety. They typically make up $10\% - 20\%$ of the total population and are jointly composed of discoverers and joiners. Their position update formula is as follows:

$$X_{i,j}^{t+1} = \begin{cases} X_{\text{best }}^{t} + \beta \cdot \left|X_{i,j}^{t} - X_{\text{best }}^{t+1}\right|, f_i > f_g \\ X_{i,j}^{t} + K \cdot \left(\frac{\left|X_{i,j}^{t} - X_{\text{worst }}^{t}\right|}{(f_i - f_\omega) + \varepsilon}\right), f_i = f_g \end{cases}, \tag{3}$$

in the Equation (3), X_{best}^t represents the individual's position with the best fitness value at the current wandering, β is a normal distribution random number with mean 0 and variance 1, representing the step control coefficient. $K \in [-1, 1]$ is a random number, f_i is the current individual fitness value, f_g and f_ω represent the fitness values of the current optimal individual and the worst individual, respectively, ε is the minimum constant to prevent the denominator from being zero.

The procedure of the Sparrow Search Algorithm is as follows:

Step 1: Firstly, the location of the sparrow population is initialized randomly in the feasible search space. Set the warning value, the maximum number of iterations, the proportion of discoverers and other related parameters.

Step 2: The fitness value of the initial sparrow population was calculated. Sparrows with better fitness values were found as discoverers, and sparrows with worse fitness values were seen as adders.

Step 3: The place updating formula updated individuals' positions.

Step 4: Obtain the updated positions of all sparrows.

Step 5: Compare the fitness values of the updated positions with the previous ones. If the fitness value improves, replace the previous position with the updated one; otherwise, keep the previous position.

Step 6: Judge whether the algorithm reaches the iteration termination condition or the maximum number of iterations. If it goes the situation, proceed to the next step; otherwise, skip to step 3 to continue the iteration.

Step 7: The globally optimal fitness value and the globally optimal individual sparrow position were recorded and output.

2.2. **Wind turbine system Model.** A physical model of a wind power generation system has been developed by examining the aerodynamic features of wind turbines. The system comprises a wind turbine, a transmission mechanism, a generator, a variable-pitch actuator, and a control system. The wind turbine is responsible for transforming captured wind energy into mechanical energy. Through an analysis of the aerodynamic characteristics, a mathematical model for the wind turbine can be derived as follows:

$$\begin{cases} P_m = \frac{1}{2}\rho\pi R^2 V^3 C_p(\lambda, \beta) \\ T_m = \frac{P_m}{\omega_m} \end{cases} \tag{4}$$

in the Equation (4), P_m, which stands for wind turbine mechanical power; ρ, which represents air density; R, which represents blade length; V, which means wind speed; ω_m, which represents wind turbine rotational speed; T_m, which represents wind turbine mechanical torque. Additionally, $C_p(\lambda, \beta)$ represents the wind energy utilization coefficient, which measures the ability of wind turbines to generate electricity from wind energy. In engineering, empirical methods are commonly used to fit the wind energy utilization coefficient curve.

$$C_p(\lambda, \beta) = (0.44 - 0.0167\beta)\sin\left[\frac{\pi(\lambda - 3)}{15 - 0.3\beta}\right] - 0.00184(\lambda - 3)\beta, \tag{5}$$

in the Equation (5), β, which denotes the pitch angle and represents the angle between the wind turbine blades and the rotor plane; and λ, which means the tip velocity ratio and is defined as the ratio of tip linear velocity to wind speed.

$$\lambda = \frac{R\omega_m}{V}. \tag{6}$$

In a wind power system, the transmission system is responsible for converting the rotation of the wind turbine into the rotation of the generator, which generates electricity.The wind turbine rotates slowly due to the wind energy and is accelerated by the gearbox and transmitted to the generator side. The generator turns quickly due to the mechanical energy and generates electricity.

$$\left(J_m + k^2 J_g\right) \frac{d\omega_m}{dt} = T_m - kT_g, \tag{7}$$

in the Equation (7), J_m, which represents the wind turbine's moment of inertia; J_g, which represents the generator moment of inertia; k, which denotes the gear transmission ratio and can be expressed as $k = \omega_g/\omega_m$, where ω_m represents the wind turbine rotational speed,and ω_g represents the generator's rotational speed; T_m, which represents the wind turbine's mechanical torque and T_g, which represents the generator's electromagnetic torque.

A generator is a device that transforms mechanical energy into electrical energy. In this paper, a three-phase asynchronous generator has been selected as the focus of the study. Under optimal conditions, the mathematical model for the generator can be represented as follows:

$$\begin{cases} T_g = \frac{pmu^2 r_2}{(\omega_g - \omega_0)\left[\left(r_1 - \frac{c_1 r_2 \omega_0}{\omega_g - \omega_0}\right)^2 + (x_1 + c_1 x_2)^2\right]} \\ P_g = \omega_g T_g \end{cases}, \tag{8}$$

in the Equation (8), T_g, which represents the generator electromagnetic torque; p, which represents the number of magnetic poles in the generator; m, which represents the number of stator phases in the generator; u, which denotes the rated voltage of the generator; ω_g, which represents the generator rotational speed; ω_0, which represents the generator synchronous speed; c_1, which represents the correction factor; r_2, which denotes the rotor winding resistance referred to the stator side; r_1, which denotes the stator winding resistance; x_2, which represents the rotor winding reactance referred to the stator side; x_1, which represents the stator winding reactance; and P_g, which represents the generator output power.

The pitch control mechanism is the actuator that controls the wind turbine blades rotation angle. Due to the fatigue effect of the unit load, the pitch execution mechanism should set a reasonable interval limit for the pitch range and rate. Generally, the allowable range of blade rotation angle is between $2\,^\circ$ and $90\,^\circ$, and the pitch maximum rate of change should not exceed $10\,^\circ/s$. The mathematical models of these systems can be represented as:

$$\frac{\beta}{\beta_r} = \frac{1}{\tau s + 1}, \tag{9}$$

in the Equation (9), τ, which represents the time constant, β_r, which denotes the predetermined pitch angle, and β, which represents the current actual pitch angle.

The control system plays a crucial role in the overall design. As wind speed fluctuations can cause instability in the wind turbine's power output, it is necessary to employ a controller to regulate the pitch angle. The PID (proportional-integral-derivative) controller is a commonly used solution in the wind turbine industry. The PID controller linearly combines the deviation, integral, and derivative of the difference between rated power and actual output power to calculate the desired pitch angle value. This value is then passed through the pitch Angle actuator to get the current precise pitch Angle, thereby changing the captured wind energy to stabilize the power output. The PID control part can be represented as:

$$\beta_r = K_p \left(P_{ref} - P_g\right) + K_i \int \left(P_{ref} - P_g\right) dt + K_d \frac{d}{dt} \left(P_{ref} - P_g\right), \tag{10}$$

in the Equation(10), P_{ref} represents the wind turbine generator-rated power, K_p, K_i, K_d respectively represent the PID controller proportional, integral, and derivative coefficients. Due to the computer system functioning as a sampling control mechanism, it is impossible to utilize Equation(10) directly. Instead, it is essential to convert it into discrete PID control and determine the control value based on the deviation at sampling intervals. The precise procedure for transforming the expression is as follows:

$$\begin{cases} t = kT, (k = 0, 1, 2, \ldots) \\ \int_0^t \left(P_{ref} - P_g\right) dt = T \sum\limits_{j=0}^{k} \left(P_{ref} - P_g^{jT}\right) \\ \frac{d}{dt} \left(P_{ref} - P_g\right) = \frac{\left(P_{ref} - P_g^{kT}\right) - \left(P_{ref} - P_g^{(k-1)T}\right)}{T} \end{cases}, \tag{11}$$

in the Equation (11), T represents the sampling interval, k denotes the sequence number of each sample, and P_g^{jT} refers to the value of P_g at the time jT, the continuous time t is represented by a series of sampling time points kT. Rectangular method numerical integration is employed to handle integral calculations, while the first-order backward difference is used for differential calculations. The discrete PID control component can be expressed as follows:

$$\beta_r^{kT} = K_p \left(P_{ref} - P_g^{kT}\right) + K_i T \sum_{j=0}^{k} \left(P_{ref} - P_g^{jT}\right) + K_d \frac{\left(P_{ref} - P_g^{kT}\right) - \left(P_{ref} - P_g^{(k-1)T}\right)}{T}, \tag{12}$$

in the Equation (12), β_r^{kT} represents the prescribed pitch angle at time kT.The wind turbine generator's overall structure is shown in Figure 1.

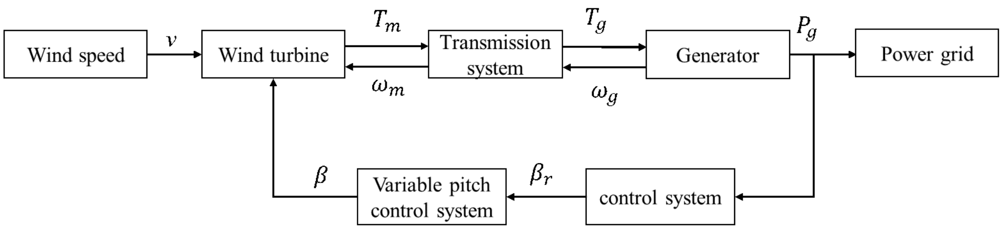

FIGURE 1. The wind turbine structure's diagram

3. Chaotic Sparrow Search Algorithm.

3.1. Tent Chaotic Mapping.

Uniform distribution of the initial population in the search space can enhance the optimization algorithm's global search performance by allowing them to integrate into the algorithm. Chaotic sequences have the characteristics of good randomness, traversability, and regularity. The basic principle is to generate chaotic sequences between [0,1] through a mapping relationship and then convert them into the search space of individuals. Compared with other mappings, Tent chaotic mapping can generate more balanced distribution sequences, Hence, this paper uses it to initialize the sparrow population. The Tent chaotic mapping's mathematical expression is as follows:

$$y_{j+1}^{i}=\left\{\begin{array}{c}\mu y_{j}^{i}, y_{j}^{i}<0.5 \\ \mu\left(1-y_{j}^{i}\right), y_{j}^{i} \geq 0.5\end{array}\right., \tag{13}$$

where $\mu \in (0, 2]$ is the chaotic parameter; i and j are the population number and the chaotic variable index, respectively.

In Equation (13), selecting multiple initial values with small differences can generate corresponding chaotic sequences y_j^i, and then convert them to the corresponding variable search space to obtain variable x_j^i

$$x_{j}^{i}=\mathrm{lb}_{i}+\left(\mathrm{ub}_{i}-\mathrm{lb}_{i}\right) y_{j}^{i}, \tag{14}$$

the symbols lb_i and ub_i in the Equation (14) denote the lower and upper limits of the variable x_j^i.

3.2. **Normal Cloud Model.** The cloud model concept was defined in 1995, which can realize the uncertain transformation between quantitative values and qualitative ideas [22]. The model can well describe and process the fuzziness and randomness of data. The normal cloud model is a mathematically significant cloud model that accurately models random probability distributions found in nature. By leveraging its inherent randomness and fuzziness, the normal cloud model can update the positions of Harris hawks in the optimization algorithm, enhancing the diversity of the population and improving the algorithm's global search performance [23]. The effectiveness of this improved algorithm was further demonstrated through the solution of a three-bar truss design problem. Another study proposed dynamically adjusting the entropy of the normal cloud model used in the fruit fly optimization algorithm during the early stages of evolution, resulting in improved global exploration capabilities for the algorithm [24].

Let C be a qualitative concept defined on a quantitative domain U, and let $x \in U$ be a random realization of the qualitative concept C. The degree of determination $u(x) \in [0, 1]$ of x to C is a stable random variable, and the membership function satisfies the equation below:

$$\mu=-\exp \left[-\frac{((x-E x))^{2}}{\left(2\left(E n^{\prime}\right)^{2}\right)}\right], \tag{15}$$

The probability distribution of the random variable X, which consists of all droplets x on the domain U, is referred to as the normal cloud model [25-27].

Figure 2 shows the correlation between the normal cloud model's digital characteristics values and the cloud droplets distribution. When the En value increases, the visible range of cloud droplet distribution will expand continuously. Simultaneously, as the He value increases, the dispersion degree will also correspondingly. These observations demonstrate the random and fuzzy nature of cloud droplet distribution. The positive normal cloud generator is an algorithm that generates droplets that follow a normal distribution. Each time it runs, it produces one droplet until it generates the expected number of droplets. The process of generating normal cloud droplets can be defined in the following form.

$$X\left[x_{1}, x_{2}, \ldots, x_{N d}\right]=\operatorname{Gnc}(E x, E n, \mathrm{He}, \mathrm{Nd}), \tag{16}$$

where Nd is the expected number of generated droplets.

3.3. **Chaotic Sparrow Search Algorithm.** To enhance the accuracy of convergence in dealing with intricate optimization problems and to improve the ability of SSA to escape from local optimal solutions, this paper presents an improved sparrow search algorithm (Chaotic Sparrow Search Algorithm with normal cloud model, referred to as CSSA)

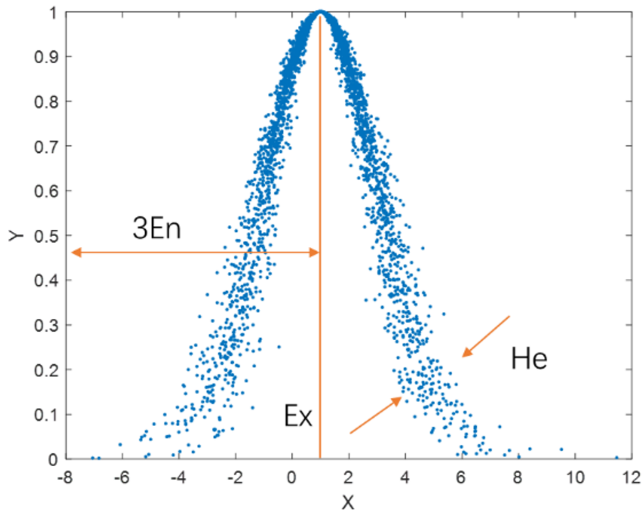

FIGURE 2. A normal cloud distribution

based on two improvement mechanisms. In the initialization stage of the population, the Tent chaotic mapping is used instead of the random number generator. In the iterative process of the population, the normal cloud model is introduced to give the sparrow population some mutation or disturbance to increase the group's vitality. More specifically, the proposed method updates the position of the current elite individual in the sparrow population by performing deep development with its position as the expected value, Ex, of the normal cloud model. The following formula is used to update the new position:

$$\text{Position}_{\text{new}} = f_{\text{cloud}}\left(\text{position}_{\text{best}},\ \text{En, He, Nd}\right), \tag{17}$$

the position of the current best individual is represented by $position_{best}$.

Thus, relative to the optimal individual, the update range of the sparrow population's position can be regulated by the En value, which determines the dispersion degree of the position update. Typically, during the early stage of the search process, the sparrows are located far from the food source, so a more comprehensive position update range can be chosen. As the search progresses and the sparrows get closer to the food source, the update range can be gradually reduced to enhance search precision.

$$En = \omega \times \left(\frac{\text{maxiter} - t}{\text{maxiter}}\right)^{\tau}, \tag{18}$$

$$He = En \times 10^{-\xi}, \tag{19}$$

where $\omega \in (0,1)$, τ, and ξ are positive integers, besides t is the current iteration number. To clearly illustrate the operation process of the improved sparrow search algorithm, we use pseudo-code Algorithm 1 to represent its steps.

Table 1. Algorithms parameters settings

Algorithm	Parameters settings
CSSA	ST=0.8, PD=0.8, SD=0.2, ω=0.3, tao=1, E=2
SSA	ST=0.8, PD=0.8, SD=0.2
PSO	N=200, $\omega_{max} = 0.9$, $\omega_{min} = 0.4$, $c_1 = c_2 = 2$, $V_{max} = 10$, $V_{min} = -10$
WOA	N=200, $l \sim U(-1,1)$, $p \sim U(0,1)$
LWOA	N=200, $l \sim U(-1,1)$, $p \sim U(0,1)$

Algorithm 1 CSSA pseudo code

1. **INPUT:***Set the basic parameters of the algorithm (set the maximum number of iterations to Tmax, the number of discoverers to P, the number of warners to S, the caution threshold to G, and the sparrow population size to n);*
2. *Initialize the population positions based on the Tent chaotic mapping mechanism; /Algorithm Iterative Search Stage/*
3. **While** *(t < Tmax)*
4. *Sort individual fitness values and find the best and worst individuals;*
5. *G = rand(1);*
6. **For** *i = 1:P*
7. *Update the position of discoverers;*
8. **End for**
9. **For** *i = P:n*
10. *Update the position of joiners;*
11. **End for**
12. **For** *i = 1:S*
13. *Update the position of warners;*
14. **End for**
15. *Select elite individuals based on the normal cloud model mechanism for mutation operations;*
16. *Evaluate the fitness value of the mutated individual. If the mutated position is better, update it as the current best position;*
17. *t = t + 1;*
18. **End while**
19. **Output:** *the global optimal solution.*

4. Experiment Results for Testing Functions.

4.1. Experimental parameter setting. In order to assess the effectiveness of the CSSA algorithm, the CEC2013 test suite was utilized in this study [16]. The CEC2013 test suite comprises complex functions appropriate for evaluating algorithm performance. The test suite comprises 28 functions, with f_1 to f_5 being single-peaked functions, f_6 to f_{20} being multi-peaked functions, and f_{21} to f_{28} being composite functions.

Due to each benchmark function having different optimal values, the optimization performance of the test algorithm cannot be intuitively reflected. Therefore, this article aims to obtain the error value $\Delta f = f_i - f_i^*$ for each benchmark function. Here, fi represents

TABLE 2. A performance for the SSA, PSO and CSSA under CEC2013

5D	SSA			PSO			**CSSA**		
	Mean	Best	Std	Mean	Best	Std	Mean	Best	Std
F1	7.22E+01	1.35E+00	1.01E+02	5.26E+00	1.06E+00	2.45E+00	**1.92E-02**	**2.30E-03**	**1.32E-02**
F2	3.42E+05	7.46E+03	4.06E+05	1.46E+05	6.34E+03	1.30E+05	**6.24E+04**	**4.15E+03**	**6.71E+04**
F3	6.18E+07	8.08E+05	9.89E+07	3.84E+06	6.86E+05	**4.28E+06**	**3.70E+06**	**1.47E+03**	6.78E+06
F4	1.01E+04	**9.79E+02**	6.15E+03	8.58E+03	1.16E+03	4.46E+03	**5.99E+03**	2.27E+03	**2.29E+03**
F5	3.80E+01	9.75E-01	2.74E+01	**4.05E+00**	1.04E+00	**1.94E+00**	6.55E+00	**9.22E-03**	1.44E+01
F6	**2.05E+00**	**2.90E-02**	1.83E+00	2.81E+00	8.42E-02	2.06E+00	3.18E+00	3.93E-02	**1.48E+00**
F7	1.30E+01	1.02E+00	1.25E+01	5.86E+00	1.09E+00	4.36E+00	**5.00E+00**	**1.69E-01**	**2.94E+00**
F8	1.88E+01	2.90E+00	3.61E+00	1.96E+01	7.03E+00	2.68E+00	**1.63E+01**	**1.64E+00**	6.52E+00
F9	1.98E+00	5.31E-01	**7.30E-01**	2.17E+00	8.33E-01	8.21E-01	**1.33E+00**	**2.18E-01**	8.82E-01
F10	1.90E+01	6.85E-01	2.15E+01	1.89E+00	1.03E+00	**5.69E-01**	**1.47E+00**	**3.20E-01**	9.02E-01
F11	1.21E+01	1.28E+00	5.83E+00	1.15E+01	3.68E+00	4.52E+00	**5.20E+00**	**1.02E+00**	**2.21E+00**
F12	1.44E+01	4.74E+00	7.76E+00	1.31E+01	3.39E+00	5.08E+00	**7.97E+00**	**1.03E+00**	**4.86E+00**
F13	1.58E+01	5.45E+00	7.89E+00	1.28E+01	4.51E+00	**5.38E+00**	**9.19E+00**	**1.59E+00**	5.76E+00
F14	2.19E+02	5.50E+01	1.21E+02	4.37E+02	7.48E+01	1.68E+02	**1.00E+02**	**7.40E-01**	**7.26E+01**
F15	3.37E+02	2.39E+01	**1.22E+02**	4.95E+02	1.24E+02	1.87E+02	**2.64E+02**	**1.49E+01**	1.64E+02
F16	6.66E-01	3.83E-01	1.95E-01	1.78E+00	8.37E-01	4.61E-01	**4.88E-01**	**1.53E-01**	**1.48E-01**
F17	1.40E+01	**6.18E+00**	5.17E+00	1.64E+01	6.49E+00	4.50E+00	**1.22E+01**	6.69E+00	**3.17E+00**
F18	1.35E+01	**5.54E+00**	4.53E+00	1.90E+01	9.85E+00	3.94E+00	**1.16E+01**	8.06E+00	**3.18E+00**
F19	1.46E+00	2.31E-01	1.11E+00	1.06E+00	4.99E-01	**2.95E-01**	**9.87E-01**	2.17E-01	5.03E-01
F20	7.96E-01	2.37E-01	3.57E-01	1.03E+00	**1.96E-01**	**3.29E-01**	**6.96E-01**	2.32E-01	3.76E-01
F21	3.18E+02	1.23E+02	9.32E+01	2.94E+02	1.30E+02	**5.31E+01**	**2.76E+02**	**1.02E+02**	6.83E+01
F22	4.71E+02	**9.66E+01**	1.77E+02	7.72E+02	4.16E+02	1.63E+02	**3.49E+02**	1.48E+02	**9.45E+01**
F23	5.24E+02	**1.57E+02**	**1.50E+02**	6.43E+02	3.39E+02	2.10E+02	**4.59E+02**	1.61E+02	1.75E+02
F24	1.51E+02	9.69E+01	3.57E+01	1.38E+02	**5.95E+01**	3.98E+01	**1.21E+02**	7.84E+01	**1.29E+01**
F25	1.29E+02	1.08E+02	2.88E+01	1.18E+02	1.09E+02	6.92E+00	**1.12E+02**	**1.00E+02**	**6.12E+00**
F26	1.30E+02	2.52E+01	4.35E+01	1.24E+02	6.55E+01	3.30E+01	**9.92E+01**	**2.27E+00**	**2.07E+01**
F27	3.64E+02	**1.84E+02**	4.27E+01	3.62E+02	3.18E+02	2.76E+01	**3.47E+02**	2.82E+02	3.25E+01
F28	3.22E+02	1.27E+02	8.19E+01	3.09E+02	**6.49E+01**	9.30E+01	**2.90E+02**	1.01E+02	**5.25E+01**
Win	27	21	23	27	23	21	---	---	---
Lose	1	7	5	2	5	7	---	---	---
Draw	0	0	0	0	0	0	---	---	---

the actual value of the i-th benchmark function, and fi represents its optimal value. A smaller error value indicates a better optimization result. The experiments were conducted in MATLAB R2020b on a computer with an Intel(R) Core(TM) i5-10400F CPU @ 2.90GHz 2.90 GHz.

The performance of the CSSA algorithm was evaluated and compared with standard algorithms such as PSO, WOA, SSA, and an improved algorithm (LWOA) on various benchmark functions to verify its effectiveness. A consistent environment was set for all testing algorithms to ensure fairness in the experiments. The maximum evaluation number was 1500 times, and the initial population or virtual population size was set to 50, with a dimension of 5 for individuals. To minimize experimental randomness, 30 experiments were conducted for all testing algorithms, providing more objective results. Table 1 shows the primary parameter settings for each algorithm.

4.2. **Experimental Results and Analysis with Test Functions.** This paper assesses the performance of various algorithms using mean value, best value, and standard deviation. Tables 2 and 3 show the results of various algorithms running on different benchmark functions [29-33]. The analysis of data in Table 2 indicates that, in comparison to SSA, CSSA obtained better mean values in 90% of the functions, better best values in 80% of the functions, and better standard deviations in 80%. Compared with PSO, CSSA achieved better mean values in 90% of the functions, better best values in 80% of the

TABLE 3. A performance for WOA, LWOA and CSSA under CEC2013

5D	WOA			LWOA			**CSSA**		
	Mean	Best	Std	Mean	Best	Std	Mean	Best	Std
F1	1.57E+01	1.19E+00	1.26E+01	9.70E-01	7.23E-02	7.12E-01	**1.92E-02**	**2.30E-03**	**1.32E-02**
F2	2.68E+06	3.48E+04	3.11E+06	1.42E+06	1.32E+04	2.43E+06	**6.24E+04**	**4.15E+03**	**6.71E+04**
F3	6.04E+07	2.83E+05	8.97E+07	3.40E+07	4.86E+04	5.99E+07	**3.70E+06**	**1.47E+03**	**6.78E+06**
F4	2.12E+04	4.31E+03	1.37E+04	2.19E+04	3.39E+03	1.27E+04	**5.99E+03**	**2.27E+03**	**2.29E+03**
F5	9.64E+01	7.27E+00	9.64E+01	1.84E+01	4.07E-01	2.13E+01	**6.55E+00**	**9.22E-03**	**1.44E+01**
F6	1.74E+01	1.04E+00	3.66E+01	5.64E+00	9.77E-02	1.38E+01	**3.18E+00**	**3.93E-02**	**1.48E+00**
F7	2.18E+01	4.45E+00	1.43E+01	1.38E+01	1.67E+00	1.02E+01	**5.00E+00**	**1.69E-01**	**2.94E+00**
F8	2.02E+01	2.00E+01	**1.15E-01**	1.97E+01	4.33E+00	2.91E+00	**1.63E+01**	**1.64E+00**	6.52E+00
F9	2.79E+00	9.55E-01	8.51E-01	2.40E+00	5.30E-01	9.41E-01	**1.33E+00**	**2.18E-01**	**8.82E-01**
F10	3.31E+01	2.21E+00	2.82E+01	8.60E+00	1.08E+00	7.96E+00	**1.47E+00**	**3.20E-01**	**9.02E-01**
F11	2.08E+01	6.10E+00	1.06E+01	1.69E+01	3.29E+00	1.11E+01	**5.20E+00**	**1.02E+00**	**2.21E+00**
F12	2.24E+01	6.88E+00	1.11E+01	2.03E+01	5.48E+00	1.39E+01	**7.97E+00**	**1.03E+00**	**4.86E+00**
F13	2.36E+01	2.02E+00	1.22E+01	1.87E+01	6.39E+00	7.65E+00	**9.19E+00**	**1.59E+00**	**5.76E+00**
F14	3.81E+02	7.41E+01	1.91E+02	4.50E+02	3.67E+01	1.98E+02	**1.00E+02**	**7.40E-01**	**7.26E+01**
F15	5.61E+02	2.21E+02	1.54E+02	4.05E+02	2.68E+01	1.68E+02	**2.64E+02**	**1.49E+01**	1.64E+02
F16	1.19E+00	3.48E-01	3.69E-01	1.68E+00	8.62E-01	4.32E-01	**4.88E-01**	**1.53E-01**	**1.48E-01**
F17	2.77E+01	1.21E+01	9.23E+00	2.22E+01	8.21E+00	8.19E+00	**1.22E+01**	**6.69E+00**	**3.17E+00**
F18	2.86E+01	1.10E+01	1.10E+01	2.81E+01	6.77E+00	1.01E+01	**1.16E+01**	**8.06E+00**	**3.18E+00**
F19	2.18E+00	4.49E-01	1.55E+00	1.40E+00	**1.02E-01**	8.72E-01	**9.87E-01**	2.17E-01	**5.03E-01**
F20	1.22E+00	4.24E-01	3.66E-01	1.25E+00	6.00E-01	3.42E-01	**6.96E-01**	**2.32E-01**	3.76E-01
F21	3.76E+02	1.16E+02	1.50E+02	3.10E+02	1.09E+02	1.05E+02	**2.76E+02**	**1.02E+02**	**6.83E+01**
F22	7.51E+02	3.51E+02	2.13E+02	6.75E+02	3.78E+02	1.84E+02	**3.49E+02**	**1.48E+02**	**9.45E+01**
F23	7.57E+02	4.46E+02	1.76E+02	7.16E+02	2.32E+02	2.53E+02	**4.59E+02**	**1.61E+02**	**1.75E+02**
F24	1.56E+02	1.04E+02	4.02E+01	1.70E+02	1.12E+02	4.01E+01	**1.21E+02**	**7.84E+01**	**1.29E+01**
F25	1.29E+02	1.07E+02	1.90E+01	1.32E+02	1.10E+02	2.38E+01	**1.12E+02**	**1.00E+02**	**6.12E+00**
F26	1.45E+02	1.04E+02	3.81E+01	1.35E+02	6.55E+01	3.89E+01	**9.92E+01**	**2.27E+00**	**2.07E+01**
F27	3.86E+02	3.14E+02	**2.56E+01**	3.77E+02	3.17E+02	3.04E+01	**3.47E+02**	**2.82E+02**	3.25E+01
F28	3.30E+02	1.52E+02	7.22E+01	3.03E+02	1.10E+02	9.49E+01	**2.90E+02**	**1.01E+02**	**5.25E+01**
Win	28	28	24	28	26	25	---	---	---
Lose	0	0	4	0	2	3	---	---	---
Draw	0	0	0	0	0	0	---	---	---

TABLE 4. The parameters value range be optimized

Parameters	Search Range
K_p	0~5000
K_i	0~5000
K_d	0~5000

functions, and better standard deviations in 80%. The results in Table 3 show that compared with WOA and LWOA, SSA achieved better mean and best values in over 90% of the benchmark functions, and better standard deviation in over 80% of the functions.

The CSSA algorithm outperforms the SSA, PSO, WOA, and LWOA algorithms on the CEC2013 test functions, particularly in terms of mean, best, and standard deviation values. To further illustrate the performance of the algorithms, the convergence curves of six benchmark functions are shown in Figure 3. The results demonstrate that CSSA exhibits superior optimization performance, achieving better accuracy and faster convergence than the original SSA algorithm. The data in Tables 2 and 3 corroborate these findings, indicating that CSSA performs better than the other algorithms.

The standard Sparrow Search Algorithm (SSA) is a new metaheuristic algorithm, but it has slow convergence and can become stuck in local optima. To address these issues,

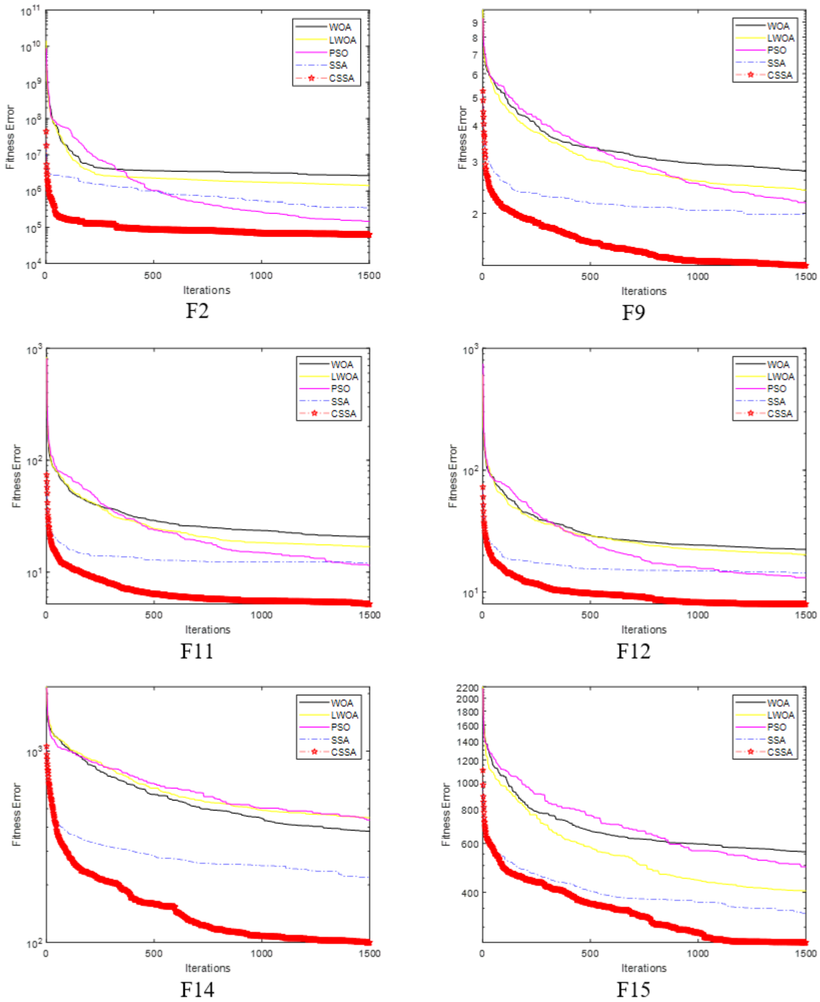

FIGURE 3. A comparison of the best fitness curves selected functions with 5D optimization

TABLE 5. The parameters of wind turbine

Parameters	Values
Rated power of the generator	3MW
Rated speed of the wind turbine	3m/s
Rated wind speed	12m/s
Cut-in wind speed	3m/s
Cut-out wind speed	25m/s
Moment of inertia of the wind turbine	6250000kg·m^2
Moment of inertia of the generator	15kg·m^2
Gear ratio	80
Range of pitch angle adjustment	0~30°
The maximum rate of pitch angle change	10°/s

this paper proposes a modified version called the CSSA algorithm, which incorporates the Tent chaotic mapping mechanism and the normal cloud model. The performance of the CSSA algorithm is evaluated on benchmark functions and compared to that of the SSA, PSO, WOA, and LWOA algorithms. The results demonstrate that the proposed algorithm achieves good optimization performance.

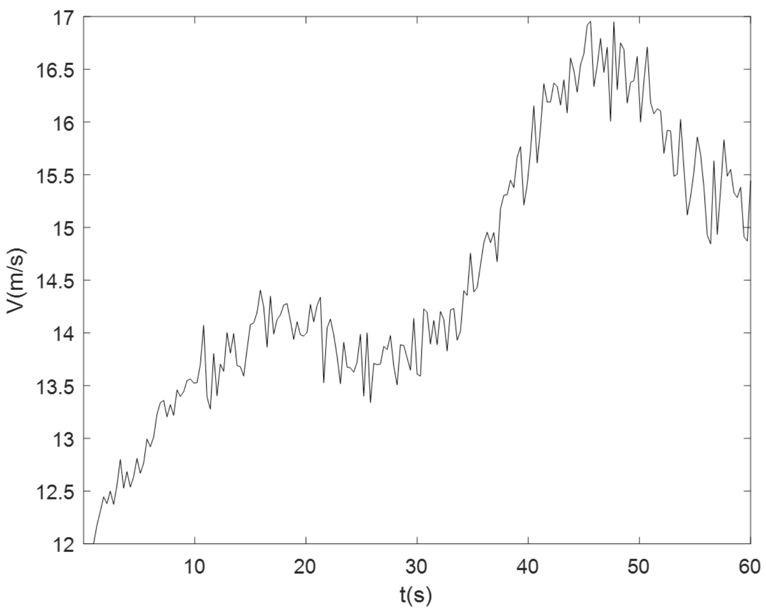

FIGURE 4. The wind speed's changing curve

5. **Wind Turbine Pitch Control Using CSSA.** This section consists of the subsections of the experimental parameter settings for environment and experimental results and analysis.

5.1. **Experimental Parameter Settings.** In wind power generation, the random fluctuation of wind speed affects the power output, resulting in instability [13]. Therefore, variable pitch control is crucial to maintain stable power output. Currently, the PID controller is the most widely used control mechanism for variable pitch control, which has three main control parameters: K_p, K_i, and K_d. However, the traditional PID parameter setting method cannot meet the control requirements well, leading to the need for secondary adjustment based on the designer's experience, making the design of the variable pitch control mechanism more complicated. To address these issues, this study proposes using CSSA to adjust the PID parameters, which can save time in manual parameter adjustment, improve the control accuracy and speed of the system, and overcome the limitations of traditional adjustment methods [14]. The range of optimization parameters is pre-defined based on design experience, as shown in Table 4.

In order to better assess the stability of the system's output power, this study employs the Integral of Time multiplied by the Absolute Error (ITAE) criterion as the fitness function. ITAE is a practical and selective evaluation criterion for control system performance. The fitness function F is represented explicitly as:

$$F = \int t|e(t)|dt, \tag{20}$$

where $e(t)$ represent the error in the system between the actual and rated power output. The objective function is more minor, and the system's power output is more stable.

The Matlab/Simulink simulation software was used in this study to verify the model and algorithm effectiveness. Table 5 displays the generator set for the wind turbine parameters, and Figure 4 presents the curve depicting the wind speed fluctuations.

5.2. **Experimental results and analysis.** Using the parameter settings mentioned above, the experiment can obtain the wind turbine generator's convergence curve, power

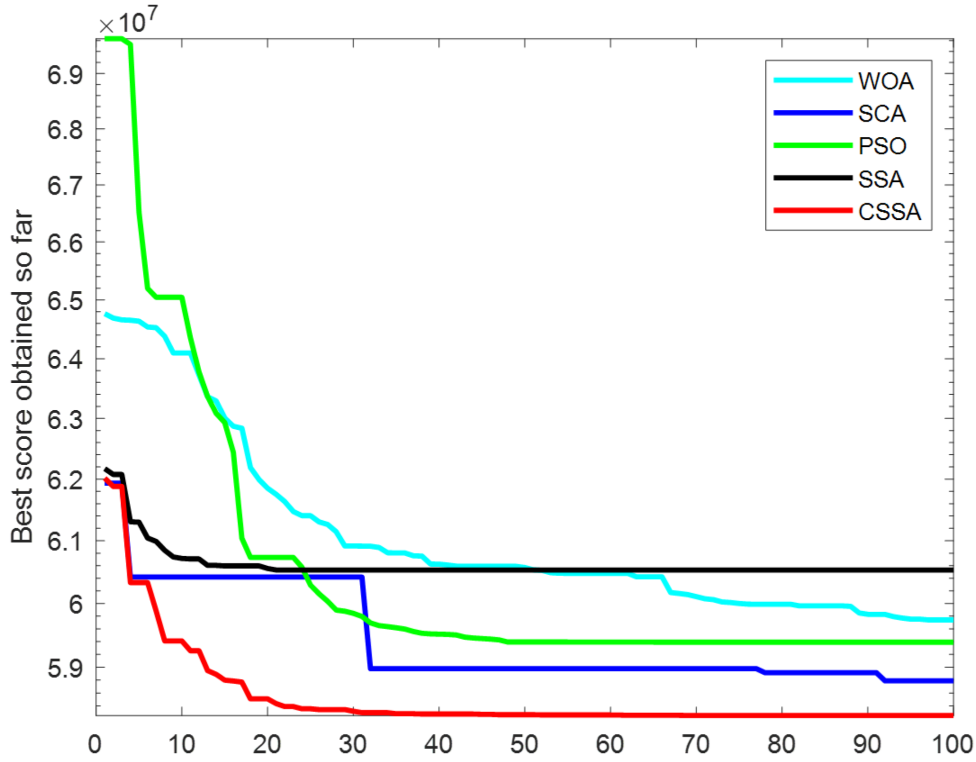

FIGURE 5. Comparison of the proposed algorithm with the other methods for the convergence curve of wind turbine

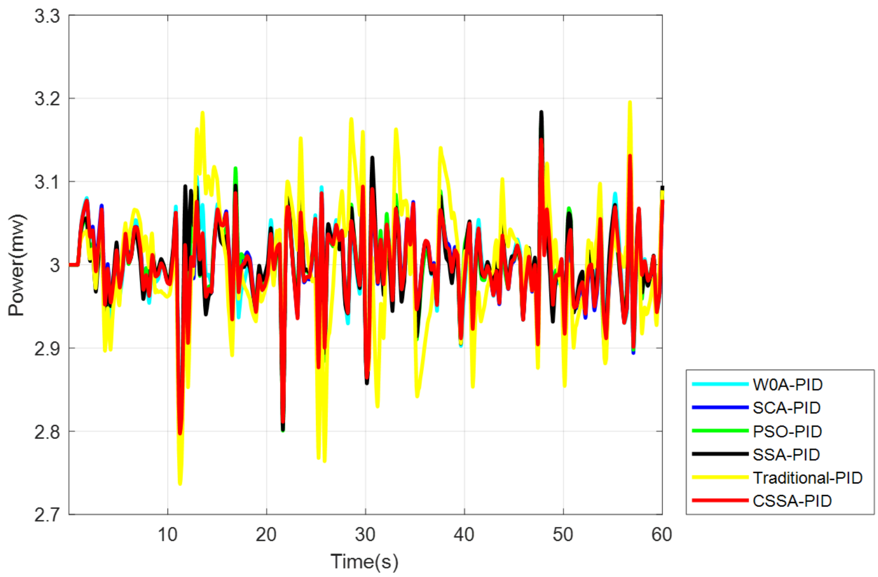

FIGURE 6. An example of a real closed house used in actual mapping construction

curve, parameter tuning values, and objective function value. The obtained convergence curve indicates that the proposed CSSA algorithm outperforms other algorithms, achieving better accuracy and faster convergence during optimization.

To assess the power curve's performance objectively, this study evaluates it using five performance indicators: average value, maximum value, maximum fluctuation range, variance, and pitch angle rotation range. These performance indicators are presented in Table 7. The results from Figure 7 and Tables 6 and 7 reveal that the metaheuristic

Table 6. The Optimization results of PID parameters

	K_p	K_i	K_d	F
WOA-PID	69.3528	70.3504	86.3955	5.9740e+07
SCA-PID	61.5944	88.6206	84.5247	5.8789e+07
PSO-PID	39.1549	79.5143	80.9883	5.9390e+07
SSA-PID	38.8131	62.0277	86.8449	6.0531 e+07
Traditional-PID	56.0000	16.2000	31.0000	9.9377e+07
CSSA-PID	60.3870	85.5010	86.5579	5.8253e+07

Table 7. The dynamic performance indicators of statistical calculations of the schemes

Algorithm	Mean value (MW)	Maximum value (MW)	Minimum value (MW)	Maximum fluctuation (MW)	Standard deviation
WOA-PID	2.998962	3.150401	2.797137	0.353264	0.019369
SCA-PID	2.998648	3.153253	2.792728	0.360525	0.019023
PSO-PID	2.999150	3.175175	2.769557	0.405618	0.020522
SSA-PID	2.999342	3.183639	2.776334	0.407305	0.021040
Traditional-PID	2.999113	3.195366	2.736602	0.458764	0.052661
CSSA-PID	2.999572	3.146975	2.810231	0.336744	0.018546

algorithm-tuned controller outperforms the traditional PID controller tuned using conventional methods in all performance indicators. This is due to the metaheuristic algorithm's faster and more stable convergence accuracy and faster convergence speed, making it easier to find appropriate PID control parameters. Furthermore, the PID control tuned by the metaheuristic algorithm outperforms the traditional PID control and eliminates the drawbacks of being time-consuming and labor-intensive.

The optimization process of CSSA shows improved accuracy and performance compared to traditional PID and other algorithms. Among the PID parameter tuning methods, CSSA performs the best. Consequently, CSSA is highly feasible in addressing the pitch control issue in wind power generation systems by achieving stable wind turbine power output and mitigating the adverse effects of wind speed fluctuations on the power grid.

6. **Conclusions.** This study proposed CSSA for the optimal parameters tuning of the variable-pitch controller of wind turbines. The CSSA algorithm was introduced by a mutation strategy based on the SSA with the Tent chaotic map for updating the sparrow population's initial distribution and position and the normal cloud model, which avoids the drawbacks of slow convergence and insufficient optimization accuracy of the SSA algorithm. The performance improvement of the CSSA scheme was validated by comparing it with the SSA, PSO, WOA, and LWOA on the CEC2013 test suite. The experimental results show that CSSA achieves good results compared to other methods in solving the variable-pitch control problem of wind power generation systems. The results show that the CSSA algorithm in the control process can reduce power fluctuations, shorten the time to recover to stability, and output power closer to the rated power than other methods. The CSSA performs excellently on the test suite and demonstrates superior ability in parameter tuning the variable-pitch controller of wind turbines, improving wind

turbine units' stability. In future work, the suggested CSSA will be applied to optimal routing, sensing, and authentication schemes [34,35].

7. **Acknowledgments.** This work was supported in part by Fujian Provincial Department of Science and Technology under Grant No. 2021J011070, and Fujian University of Technology under Grant No. GY-Z18148.

REFERENCES

[1] T. T. Nguyen, T. G. Ngo, T. K. Dao, and T. T. T. Nguyen, "Microgrid Operations Planning Based on Improving the Flying Sparrow Search Algorithm," *Symmetry*, vol. 14, no. 1, 168, 2022.

[2] Z. Quan, L. Quan, and J. Zhang, "Review of energy efficient direct pump controlled cylinder electro-hydraulic technology," *Renewable and Sustainable Energy Reviews*, vol. 35, pp. 336–346, 2014.

[3] A. Gambier, "Pitch control of three bladed large wind energy converters—a review," *Energies*, vol. 14, no. 23, 8083, 2021.

[4] T.-T. Nguyen, H.-J. Wang, T.-K. Dao, J.-S. Pan, J.-H. Liu, and S.-W. Weng, "An Improved Slime Mold Algorithm and Its Application for Optimal Operation of Cascade Hydropower Stations," *IEEE Access*, vol. 8, pp. 226754 - 226772, 2020.

[5] M.-H. Chiang, "A novel pitch control system for a wind turbine driven by a variable-speed pump-controlled hydraulic servo system," *Mechatronics*, vol. 21, no. 4, pp. 753–761, 2011.

[6] J.-S. Pan, T.-L.-P. Nguyen, T.-G. Ngo, T.-T.-T. Nguyen. T.-K. Dao, and T.-T. Nguyen, "An Optimizing Cross-Entropy Thresholding for Image Segmentation based on Improved Cockroach Colony Optimization," *Journal of Information Hiding and Multimedia Signal Processing*, vol. 11, no. 4, pp. 162–171, 2020.

[7] T. T. Nguyen, J. S. Pan, and T. K. Dao, "A novel improved bat algorithm based on hybrid parallel and compact for balancing an energy consumption problem," *Information (Switzerland)*, vol. 10, no. 6, 194, 2019.

[8] Z. Chen, J. M. Guerrero, and F. Blaabjerg, "A review of the state of the art of power electronics for wind turbines," *IEEE Transactions on Power Electronics*, vol. 24, no. 8, pp. 1859–1875, 2009.

[9] T. Dao, T. Nguyen, J. Pan, Y. Qiao, and Q. Lai, "Identification Failure Data for Cluster Heads Aggregation in WSN Based on Improving Classification of SVM," *IEEE Access*, vol. 8, pp. 61070–61084, 2020.

[10] T. T. Nguyen, M. J. Wang, J. S. Pan, T. kien Dao, and T. G. Ngo, "A Load Economic Dispatch Based on Ion Motion Optimization Algorithm," *in Smart Innovation, Systems and Technologies*, vol. 157, pp. 115–125, 2020.

[11] T.-T. Nguyen, T.-K. Dao, M.-F. Horng, and C.-S. Shieh, "An Energy-based Cluster Head Selection Algorithm to Support Long-lifetime in Wireless Sensor Networks," *Journal of Network Intelligence*, vol. 01, no. 01, pp. 23–37, 2016.

[12] T.-K. Dao, T.-T. Nguyen, V.-T. Nguyen, and T.-D. Nguyen, "A Hybridized Flower Pollination Algorithm and Its Application on Microgrid Operations Planning," *Applied Sciences*, vol. 12, no. 13, pp. 6487, 2022.

[13] F. Garelli, P. Camocardi, and R. J. Mantz, "Variable structure strategy to avoid amplitude and rate saturation in pitch control of a wind turbine," *International Journal of Hydrogen Energy*, vol. 35, no. 11, pp. 5869–5875, 2010.

[14] B. Zhang, S. You, M. Liu, and X. Zhou, "Design and Parameter Tuning of Nonlinear Active Disturbance Rejection Controller for Permanent Magnet Direct Drive Wind Power Converter System," *IEEE Access*, vol. 9, pp. 33836-33848, 2021.

[15] J. Xue and B. Shen, "A novel swarm intelligence optimization approach: sparrow search algorithm," *Systems Science & Control Engineering*, vol. 8, no. 1, pp. 22–34, 2020.

[16] F. S. Gharehchopogh, M. Namazi, L. Ebrahimi, and B. Abdollahzadeh, "Advances in sparrow search algorithm: a comprehensive survey," *Archives of Computational Methods in Engineering*, vol. 30, no. 1, pp. 427–455, 2023.

[17] T.-Y. Wu, Y.-Q. Lee, C.-M. Chen, Y. Tian, and N. A. Al-Nabhan, "An enhanced pairing-based authentication scheme for smart grid communications," *Journal of Ambient Intelligence and Humanized Computing*, 2021, doi.org/10.1007/s12652-020-02740-2

[18] T.-K. Dao, S.-C. Chi, T.-T. Nguyen, T.-D. Nguyen, and V.-T. Nguyen, "An Optimal WSN Node Coverage Based on Enhanced Archimedes Optimization Algorithm," *Entropy*, vol. 24, no. 8, 1018, 2022.

[19] T.-Y. Wu, C. M Chen, K. H. Wang, J. S. Pan, W. Zheng, S. C. Chu, and J. F. Roddick, "Security Analysis of Rhee et al.'s Public Encryption with Keyword Search Schemes: A Review," *Journal of Network Intelligence*, vol. 3, no. 1, pp. 16–25, 2018.

[20] H. A. A. Mansour, "Implementation of Chaotic Sequences on UWB Wireless Communication in Presence of NBI," *Journal of Information Hiding and Multimedia Signal Processing*, vol. 12, no. 2, pp. 82–92, 2021.

[21] X. Yi, "Hash function based on chaotic tent maps," *IEEE Transactions on Circuits and Systems II: Express Briefs*, vol. 52, no. 6, pp. 354–357, 2005.

[22] S. H. Wu, H. L. Chao, C. H. Ko, S. R. Mo, C. T. Jiang, T. L. Li, and C. F. Liang, "A cloud model and concept prototype for cognitive radio networks," *IEEE Wireless Communications*, vol. 19, no. 4, pp. 49–58, 2012.

[23] I. Attiya, M. A. Elaziz, and S. Xiong, "Job Scheduling in Cloud Computing Using a Modified Harris Hawks Optimization and Simulated Annealing Algorithm," *Computational Intelligence and Neuroscience*, vol. 2020, no. 16, pp. 1–17, 2020.

[24] L. Wu, C. Zuo, and H. Zhang, "A cloud model based fruit fly optimization algorithm," *Knowledge-Based Systems*, vol. 89, no. 10, pp. 603–617, 2015.

[25] C. M. Chen, Y. R. Hao, T. Y. Wu, Discussion of "Ultra Super Fast Authentication Protocol for Electric Vehicle Charging Using Extended Chaotic Maps", *IEEE Transactions on Industry Applications*, vol. 59, no. 2, pp. 2091-2092, 2023.

[26] T. Y. Wu, A. K. Shao, and J.-S. Pan, CTOA: Toward a Chaotic-Based Tumbleweed Optimization Algorithm, *Mathematics* , vol. 11, no. 10, 2339, 2023.

[27] T. Y. Wu, H. N. Li, and S.-C. Chu, CPPE: An Improved Phasmatodea Population Evolution Algorithm with Chaotic Maps, *Mathematics* , vol. 11, no. 9, 1977, 2023.

[28] S. M. Chen, C.-H. Wang, Z. Y. Dong, Q. G. Zhao, Q. P. Yang, Y. Wei and G. S. Huang, "Performance Evaluation of Three Intelligent Optimization Algorithms for Obstacle Avoidance Path Planning," *Proceedings of the 14th International Conference on Genetic and Evolutionary Computing, Jilin, China, Lecture Notes in Electrical Engineering*, vol. 833, pp. 60–69, 2022.

[29] C.-H, Wang, S. Chen, Q.Zhao, and Y. Suo, "An Efficient End-to-End Obstacle Avoidance Path Planning Algorithm for Intelligent Vehicles Based on Improved Whale Optimization Algorithm," *Mathematics*, vol. 11, no. 8, 1800, 2023.

[30] Z. Y. Dong, C.-H. Wang, Q. G. Zhao, Y. Wei, S. M. Chen, and Q. P. Yang, "A Study on Intelligent Optimization Algorithms for Capacity Allocation of Production Networks." *Proceedings of 2021 Chinese Intelligent Systems Conference , Fuzhou, China, October 16-17, 2021. Lecture Notes in Electrical Engineering*, vol. 804, pp. 734-743, 2022.

[31] C.-H. Wang, C. J. Lee and X. J. Wu,"A Coverage-Based Location Approach and Performance Evaluation for the Deployment of 5G Base Stations." *IEEE Access*, vol. 8, pp. 123320-123333, 2020.

[32] C.-H. Wang, T.-T. Nguyen, J.-S Pan and T.-K. Dao, "An Optimization Approach for Potential Power Generator Outputs Based on Parallelized Firefly Algorithm." *Advances in Intelligent Information Hiding and Multimedia Signal Processing*, vol. 64, pp. 297-306, 2016.

[33] C. M. Chen, Shi Lv, J. R. Ning, J. M.-T. Wu,"A Genetic Algorithm for the Waitable Time-Varying Multi-Depot Green Vehicle Routing Problem", *Symmetry*, vol. 15, no. 1, 124, 2023.

[34] A. L. H. P. Shaik, M. K.Manoharan, A. K. Pani, R. R. Avala, C. M. Chen, "Gaussian Mutation–Spider Monkey Optimization (GM-SMO) Model for Remote Sensing Scene Classification", *Remote Sensing*, vol. 14, no. 24, 6279, 2022.

[35] C. M. Chen, L. L. Xu, K.H. Wang, Shuai Liu, T. Y. Wu, Cryptanalysis and Improvements on Three-party-authenticated Key Agreement Protocols Based on Chaotic Maps, *Journal of Internet Technology*, vol. 19, no. 3, pp. 679-687, 2018.